sexual and asexual forms were identified which interestingly were PAS positive. The liver biopsy in one patient showed non-caseating microscopic granulomata and the PAS stain was negative. The first case was diagnosed as parasitic infection consistent with cryptosporidium and were sent for second opinion and further classification of organism to a major outside institution and the report identified the coccidial parasite as *Isospora belli* to be the causative agent.

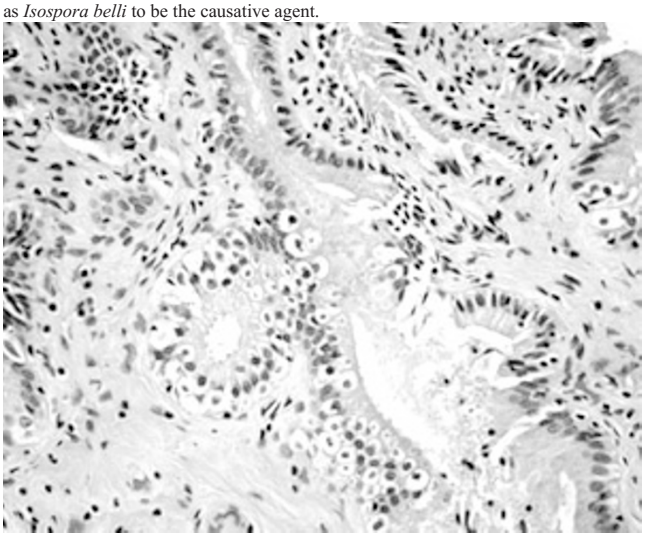

Conclusions: Significant extraintestinal complications especially cholecystitis in immunocompromised patients have been reported however to the best of our knowledge the hepatobiliary isosporiasis is not yet documented in immunocompetent patients. This report is the first and second case of isosporiasis of hepatobiliary infection in immunocompetent patients. These findings are reminders to consider the possibility of *Isospora belli* in immunocompetent patients presenting with somewhat atypical symptoms.

1495 TLR4 in Facilitating HSV-1 Neuronal Spread in Experimental Acute Retinal Necrosis (ARN) Model

M Zheng, MA Fields, Y Liu, HM Cathcart, SS Atherton. Medical College of Georgia, Augusta, GA.

Background: ARN is a rare disease usually caused by neurotropic human HSV-1. TLR4 is an innate immune mediator against a variety of pathogens, especially bacteria. Recent studies pointed toward TLR4 playing a role in a growing list of virus induced diseases.

Design: Both TLR4 mutant (mu) and wild type (wt) mice were infected with HSV-1 via anterior chamber (AC) or intravitreal inoculation. At different times post infection (p.i.), mice were sacrificed and the inoculated eyes, visual pathway containing optic nerve, chiasm, tract, and brain tissues containing the superior colliculus (SC) and lateral geniculate nucleus (LGN) were isolated. Immunohistochemistry (IHC), RT PCR, flow cytometry (FC) and virus titration were performed on the samples.

Results: Our previous results showed that after HSV-1 AC inoculation, few uninoculated, contralateral eyes of mu mice developed ARN, while ARN was observed in the majority of uninoculated eyes of wt mice. Further study revealed that an increase in certain cytokine responses at day 3 and 7 p.i. in the HSV-1 injected eye of mu compared with wt mice. FC showed more cells were infected by HSV-1 in mu compared with wt mice in virus inoculated ocular cells at day 4 p.i. One step growth curve in retinal pigment epithelial cells isolated from either mu or wt mice showed that the replication kinetics of HSV-1 were similar in both. To further investigate the role of TLR4 in virus propagation in neuronal cells within the visual pathway, HSV-1 was injected intravitreally. IHC demonstrated that HSV-1 had infected the retinal ganglion cells, then the inner nuclear cell layer cells in wt mice, whereas in mu mice, fewer cells of the subjacent retina were infected at day 2 p.i. Most HSV-1 + cells showed distinctive beta III-tubulin staining. The optic nerve was HSV-1 + at day 2 p.i. in wt mice whereas in mu mice, at day 4 p.i. The arrival of virus in the optic chiasm, tract, SC, and LGN was similarly delayed in mu compared with wt mice. IHC revealed that TLR4 was in close association with beta III-tubulin in HSV-1 infected rat retinal ganglion cells.

Conclusions: Although absence of TLR4 leads more cells to be infected by HSV-1 in virus inoculated AC, lack/delay of neuronal spread after AC or intravitreal injection of HSV-1 in mu mice suggests that TLR4 may play a role in facilitating HSV-1 transport along microtubules within the visual pathway.

Informatics

1496 Development and Use of Genitourinary Pathology Digital Teaching Set for Trainee Education and Quality Assurance

L Li, BJ Dangott, AV Parwani. Albany Medical Center, Albany, NY; University of Pittsburgh Medical Center, Pittsburgh, PA.

Background: Automated, high-speed, high-resolution whole slide imaging (WSI) robots are becoming increasingly robust and capable. This technology has started to have a significant impact on pathology practice in various aspects including resident education. Training in pathology is dependent on gaining broad exposure to these diagnostic patterns through teaching sets composed of glass slides. Whole slide imaging can provide additional educational benefits to using glass sides.

Design: A teaching set of over 250 glass slides has been used for resident education at the Division of Genitourinary Pathology, Department of Pathology, University of Pittsburgh Medical Center. Whole slide images are prepared using Aperio ScanScope CS scanner from these slides, which are de-identified. A web-based digital teaching model has been implemented at our institute using Oracle11g as the database server, SunOne as the web server, ColdFusion as the programming language, and a web middleware program to dynamically display information from a database. Case related information was obtained from electronic pathologic reports and uploaded with the corresponding whole slide images to the teaching model via a web-based data entry tool.

Results: The web site is available at: https://secure.opi.upmc.edu/genitourinary/index.cfm . It requires registration and log in. Once logged in, users can view the list of cases, and choose to show or hide the diagnoses. The search function allows searching by diagnosis or ICD-O site. A radio button is associated with each case which enables access to the case. ICD-O site, clinical history and gross description are initially shown. Whole slide images can be accessed by the links on the page that allows user to make diagnoses on their own. More information including final diagnosis will display when the diagnosis-button is clicked.

Conclusions: The web-based digital study set allows remote access to whole slide images and related information at the user's convenience. Searching and sorting functions and self-testing mode can be built in allowing more targeted study. The digital images can be annotated and the annotation can be displayed or hidden. Further, the model can be expanded to include pre-rotation and post-rotation exams, and/or to a virtual rotation system, which may potentially make standardization of pathology resident teaching possible in the future.

1497 Detection and Classification of Thyroid Follicular Lesions Based on Nuclear Structure from Histopathology Images

JA Ozolek, W Wang, GK Rohde. University of Pittsburgh, Pittsburgh, PA; Carnegie Mellon University, Pittsburgh, PA.

Background: Follicular adenoma (FA) and follicular carcinoma (FTC) are tedious challenges in surgical pathology due to lack of discriminatory cytological and microarchitectural features. Limitations of the diagnostic algorithm include time consuming tissue processing and microscopic evaluation. The aim was to develop an automated image analysis technique that could classify these lesions with 100% accuracy from routinely processed tissue using nuclear structure.

Design: Cases included 5 FA and 5 FTC resections. Sections were stained using Feulgen technique. Nuclei were segmented using random field graph cut and efficient level set active contour algorithms to yield 871 NL, 489 FA, and 703 FTC nuclei. 125 features were extracted from each nucleus. Four different classifiers (Mahalanobis distance nearest neighbors and support vector machine with different kernels) and voting strategy were used. Unique chromatin patterns were identified in feature space by finding nuclei near to each other and most distant from nuclei in other classes.

Results: These methods automatically classify the data with 100% accuracy after blind cross validation using at most 43 nuclei randomly selected from each patient.

Table 1: Classifying individual human cases using a leave one out cross validation strategy

	NL	FA	FTC
NL	10	0	0
FA	0	5	0
FTC	0	0	5

Two-dimensional representation of nuclear population with axes corresponding to directions computed by multi-dimensional scaling technique (MDS) are shown in Figure 1A (below).

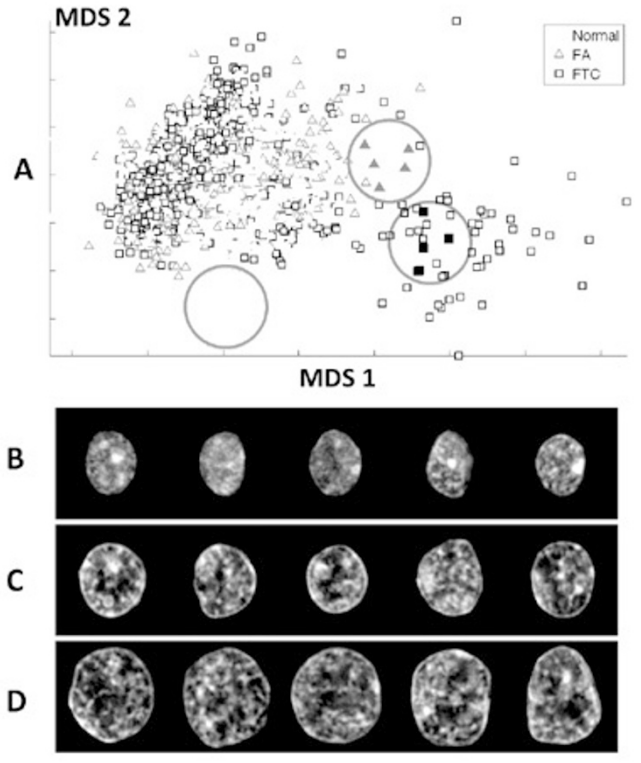

Solid shapes indicate 3 unique regions of NL, FA, and FTC nuclei (A). Nuclear representing unique regions represented in A are shown in B (NL), C (FA), D (FTC).
Conclusions: We conclude nuclear structure alone contains enough information to classify NL, FTC, and FA as long as groups of nuclei and enough features are used. The distribution of nuclear size and chromatin concentration seem to be discriminating features between NL, FA, and FTC.

1498 Building User Friendly, Searchable Databases for Meeting Abstracts

J Song, A Chang. University of Chicago, Chicago, Il.
Background: International pathology conferences, such as the annual meetings of International Academy of Pathology (IAP) and United States and Canadian Academy of Pathology (USCAP), present thousands of scientific abstracts every year. These abstracts are typically published in a supplement issue of a journal, and may also be accessible on internet. Abstracts offer an important forum to share most recent advances in pathology. However, the efficient use of abstracts has been hindered by several factors. Abstracts are not PubMed indexed; they lack references to provide background information; and they are often not searchable. In addition, it can be tedious to find out if an abstract has resulted in a full publication in peer-reviewed journal. The usability of abstracts could be greatly enhanced through data mining and transformation. The goal of our project is to build a user-friendly, searchable database for meeting abstracts.
Design: We developed a PERL computer program to automatically process abstracts complied in electronic files in PDF or HTML format. The program runs in 3 steps. (1) It parses files to retrieve the titles, authors, institutions and main texts of all abstracts. (2) For each abstract, it searches PubMed by either author names or title keywords, using the Entrez Programming Utilities. PubMed search results (articles) are retrieved in XML format, and parsed to look for keywords matching the query abstract. These articles serve as surrogate references. Multiple articles returned by a single search are sorted by the likelihood of being a true match. (3) The program creates an HTML file to display the query abstract and reference articles. Matched keywords are highlighted in colors to facilitate reading. Links to relevant online resources, such as Entrez searches and full-text articles, can be added. Finally, all batch-generated HTML files are compiled together into a file system based database. A PERL CGI interface was developed to provide the search functionality and access the database through a web server.
Results: A test database with 2005-2007 USCAP abstracts was built using this program. The database can be accessed through intranet or internet.
Conclusions: We developed software to automatically create searchable databases for abstracts. In addition to enhancing the usability of abstracts, the software can also be used to systemically analyze abstract characteristics. For example, we used the test database to quickly review all 2005-2007 USCAP abstracts, and revealed their overall publication rate (full publication in peer-reviewed journals within 3-year followup) was 36% (1725/4824).

1499 Assessment of Immunohistochemical Protein Expression in Tissue Microarrays Using Virtual Microscopic Image Analysis

TA Summers, GT Clifton, JD Gates, L Dobson, I Horkayne-Szakely, JC Shaw, A Nissan, GD Sandberg, GE Peoples, A Stojadinovic. Walter Reed Army Medical Center, Washington, DC; Brooke Army Medical Center, San Antonio, TX; SlidePath, Dublin, Ireland; Armed Forces Institute of Pathology, Washington, DC; Hadassah University Hospital Mount Scopus, Jerusalem, Israel.
Background: Interpretations of immunohistochemical (IHC) staining parameters are subjective and prone to inter- and intra-observer variability. This is highlighted by studies demonstrating that approximately 20% of HER2 analyses performed at primary treatment sites were incorrect when re-evaluated retrospectively. Virtual microscopy digitizes glass slides, therefore creating digital image environments for subsequent computer assisted interpretation of pathologic information. We provide additional evidence that Image Analysis (IA) can provide an objective analysis of IHC stain expression.
Design: Tissue microarrays (TMAs) were assembled from 160 Stage IV colon cancers metastatic to the liver (160 primary specimens, 160 metastatic liver specimens), 65 matched metastatic lymph nodes specimens, 75 normal colon specimens, and 42 transitional area specimens. TMAs were stained with MSH2 and p53. Stain expression analysis was performed by two pathologists independently and a separate uncalibrated IA was conducted using nuclear stain detection algorithms (SlidePath; Dublin, Ireland).
Results: 885 total specimens were analyzed (449-MSH2 and 436-p53). Agreement of stain expression amongst pathologists and IA was achieved for 82.3% of the specimens (729-Total; 367-MSH2, 362-p53). The individual pathologists' results were incongruent with IA in 11.6% (κ=0.767, $p<0.0005$) and 14.9% (κ=0.702, $p<0.0005$) of samples. Stain expression results between the pathologists and IA, when the pathologists agreed (807-Total), were incongruent in 9.7% of the specimens (78-Total; 37-MSH2, 41-p53; κ=0.81, p=0.054). The pathologists disagreed over stain expression for 8.8% of the specimens (78-Total; 44-MSH2, 34-p53; κ=0.83, $p<0.0005$). In the subset of specimens where pathologists disagreed, IA detected no stain expression for 80.7% of specimens (63-Total; 42-MSH2, 21-p53) suggesting over interpretation of minimal staining by the pathologists.
Conclusions: This uncalibrated study of protein expression by IA further highlights the potential of IA to increase objectivity in IHC stain interpretation and provides additional evidence that IA may fill the need for a standardized and objective assessment of clinically relevant IHC stains.

1500 Expanding the Boundaries of Digital Pathology: Application of Image Analysis as a Diagnostic Support Tool for HER2 Interpretation

Z Sun, L Dobson, KJ Kaplan. Mayo Clinic, Rochester, MN; SlidePath, Dublin, Ireland.
Background: With the development of trastuzumab, accurate evaluation of HER2 status has become particularly acute in the clinical laboratory. Although the recommended primary method of evaluation is immunohistochemistry (IHC), numerous reports of variability in interpretation have cast doubt on the reliability of HER2 testing, particularly in laboratories with a low-throughput of cases. In order to address this, recent clinical guidelines have suggested that image analysis could prove to be an effective and objective tool for achieving consistent interpretation, increasing the standard and reproducibility of assessment.
Design: This study evaluated 147 cases of invasive breast cancer with HER2 IHC stain by automated image analysis (AIA) and compared the evaluation of HER2 status with manual review by a pathologist and gene amplification status by FISH, the gold standard method of evaluation. The AIA measured several membrane stain parameters and obtained HER2 scores of 0/1 (negative), 2 (equivocal), and 3 (positive). Manual review score was made according to the ASCO/CAP scoring system where scores of 0-3+ were assigned. FISH positivity was determined by HER2/Chr17 ratio (positive >2.2, equivocal 1.8 to 2.2, and negative < 1.8).
Results: Results show that AIA could accurately determine HER2 protein expression with 94% agreement (κ = 0.73) with the pathology review across 147 cases. Eight negative cases were in complete agreement. The discrepancy was observed in 9 cases with equivocal 2+ score in either AIA or the manual review. Of the 3+ cases assigned by AIA, 95% were also found to be FISH positive. Those that were determined to be 2+ or equivocal for HER2 expression were found to be positive for gene amplification in 30% cases. Overall, an excellent concordance rate of 96% was observed between gene amplification status and AIA.
Conclusions: These results suggest that image analysis could concomitantly eliminate subjectivity and increase precision when assessing HER2 protein status in IHC stained tissue. Based on these findings, image analysis has great potential as a diagnostic support tool for pathologists and biomedical scientists, and may significantly improve the standardization of HER2 testing by providing a quantitative reference method for interpretation.

1501 Bioinformatics Solution to Unique Identification Labeling for Tissue Bank Databases: Practicing Safe "Sets"

Z vonMenchhofen, D McGarvey, V LiVolsi. University of Pennsylvania, Philadelphia, PA.
Background: Modern research approaches to human disease create a need for pathologically well-characterized human biosamples. This has led to the establishment of biological tissue banks. Various organizations, such as International Society for Biological and Environmental Repositories (ISBER), National Cancer Institute (NCI) and American Association of Tissue Banks (AATB), involved in funding and furthering research in human disease have formulated Guidelines, Recommendations and Best Practices that direct the over-arching objective mission of participating banks. These guidelines emphasize adherence to Health Insurance Portability and Accountability Act (HIPAA).

Design: The Eastern Division of the Cooperative Human Tissue Network (CHTN), an NCI sponsored prospective tissue procurement organization, has developed a programmatic informatics approach to tracking human biospecimens and data, while guaranteeing confidentiality under HIPPA. The informatic application assigns a unique identifier to each aliquot, insuring compliance with recommended Best Practices of ISBER, NCI and AATB.
Results: This set-theory approach is one of grouping individual aliquots into specialized entities for tracking and processing purposes. Each aliquot is given a unique identifier. This unique identifier is then referentially linked to one or all of the following group entities: 1) Patient Health Information Entity: denotes information about the donor. Information is kept on a secured data warehouse behind layered firewalls in an encrypted format. 2) Biosample Entity: tracks histopathologic characteristics of all the aliquots within entity. 3) Slide/Fluid Entity: references multiple quantities of individual aliquots allowing precise inventory tracking, while permitting processing of all entity member aliquots together. 4) Associative Entity: marks aliquots received from a single procedure. 5) Distribution Entity: relates all aliquots that are assigned for distribution to a single investigator. 6) Information Entity: stores digitized documentation in a secure environment, such as pathology reports, chart reviews, informed consent documents and/or slide images which pertain to an aliquot or a group of aliquots.
Conclusions: The developed application solves the question of individual aliquot labeling while preserving correlation with histopathology review procedures that guarantee proper fulfillment of investigator requests for human biosamples and data, inventory tracking, patient confidentiality, and content management documents.

1502 Use of Cloud Computing with Whole Slide Imaging for Interobserver Concordance Study

L Zhang, ST Chari, KJ Kaplan. Mayo Clinic, Rochester, MN.
Background: Pathologists routinely use glass slide concordance studies to assess interobserver agreement for specific diagnoses upon which diagnostic criteria, treatment and outcome are predicated upon. These types of studies require glass slides or necessitate pathologist travel for "multi-headed" conferences. The use of cloud computing technologies with whole slide images (WSI) allows for participants worldwide the convenience of high-resolution images virtually anytime from anywhere negating the need for transportation of glass slides or time away from clinical duties. Treatment of patients with autoimmune pancreatitis (AIP) and its various forms is highly dependent on pathological evaluation. The use of WSI remote review was performed to assess interobserver agreement.
Design: Forty cases of AIP were selected from the files of 3 study pathologists. Examples of lymphoplasmacytic sclerosing pancreatitis, idiopathic ductal centric pancreatitis, alcoholic pancreatitis and chronic obstructive pancreatitis were provided to 12 pathologists worldwide in a shared image library from to familiarize participants with the morphologic features for each entity. The cases were randomly ordered within the online library on a shared server. Images were viewable from any web-enabled PC using participants' choice of Internet browser. Slides were scanned at a central location and hosted on a cloud computing platform at no cost to study participants.
Results: The study participants reported a high level of technical satisfaction with ease of use of the site as well as image quality. No diagnoses were deferred based on image quality. Initial difficulties with account management for individual notification were resolved in a timely fashion. Questionnaire data detailing the presence of absence of 20 distinct histologic features was reviewed in real-time as participants completed reviews. The overall diagnostic agreement for the correct diagnosis amongst the 4 diagnostic categories high and comparable to glass slide diagnosis.
Conclusions: Digital pathology applications such as WSI with cloud computing allows for remote review of high quality images to be shared quickly, easily and conveniently with independent pathologist review negating the need for unnecessary courier glass slide services distant travel. Slides do not have to be returned, nor are they likely to be lost or damaged. Workflow of review of cases can be balanced and interpreted in real-time with enhanced distributed peer review.

Kidney

1503 Proliferative Glomerulonephritis with Monoclonal IgG Deposits Recurs or May Develop De Novo in Renal Allografts

A Albawardi, A Satoskar, S Brodsky, GM Nadasdy, T Nadasdy. The Ohio State University, Columbus, OH.
Background: Proliferative glomerulonephritis with monoclonal IgG deposits (PGNmIgGD) is a recently recognized glomerular disease (JASN 20:2055, 2009). The glomerular deposits are mostly IgG3 kappa and, unlike in the usual forms of monoclonal immunoglobulin deposition disease, extraglomerular deposits do not occur. The light microscopy resembles membranoproliferative glomerulonephritis (MPGN) with variable degree of glomerular lobularity/nodularity. Recurrence or de novo PGNmIgGD in renal allografts has not been reported yet.
Design: We reviewed our renal biopsy files since 01/01/03 to identify patients with PGNmIgGD in native and transplant kidney biopsies. IgG subtype staining was performed in all biopsies by immunofluorescence on frozen sections.
Results: We identified 16 patients with PGNmIgGD (0.27% of our biopsies); 3 of them have been reported previously as part of a large series (JASN 20:2055, 2009). The morphology and clinical course was similar to the previous series. The patients were mostly Caucasian females (14), had IgG3 kappa deposits (14) and had a relatively slowly progressive renal disease with severe proteinuria. Only two patients had monoclonal IgG kappa spikes in the serum; no patient had myeloma. In 15 patients, the disease appeared in the native kidney. A 68-year-old female patient had de novo disease with glomerular IgG1 kappa deposits in a renal allograft 13 years post transplant (native kidney disease was polycystic kidney disease). The graft failed 16 months following the biopsy. One patient with glomerular IgG3 kappa deposits underwent renal transplantation three years after the diagnosis of PGNmIgGD in his native kidneys. He developed recurrent disease with similar glomerular IgG3 kappa deposits one year post transplant. The patient died of a heart attack 1 ½ year after the transplant biopsy. He had 8 to 13 g/24h proteinuria and serum creatinine levels between 1.5 and 2.0 mg/dl at and after the diagnosis of recurrent disease.
Conclusions: Ours is the first report describing the appearance of PGNmIgGD in renal allografts. The disease can be de novo or recurrent. The recurrent disease developed rapidly, causing heavy proteinuria. Although based on our series we cannot determine the risk of recurrence in an individual patient, it is probably high. Our cases provide further proof that PGNmIgGD is a distinct glomerular disease entity.

1504 Primary Focal Segmental GlomerulosIcerosis Pathologic Variants in Adults and Children

M Asgari, N Bavbek, AB Fogo. Iran University of Medical Sciences, Tehran, Islamic Republic of Iran; Vanderbilt University Medical Center, Nashville, TN.
Background: The Colombia classification proposed five histopathologic variants of idiopathic Focal Segmental GlomerulosIcerosis (FSGS), namely collapsing (COLL), cellular (CELL), tip lesion variant (TIP), not otherwise specified (NOS) and perihilar (PH). Their clinical and prognostic implications have been examined in several biopsy series of adult patients, and these studies have shown worse prognosis of COLL, and better for TIP. We examined whether similar correlations were present for these different pathologic variants and their clinical characteristics and prognosis in biopsies from our practice, including both adult and children.
Design: All biopsies diagnosed as primary FSGS by LM, IF and EM in our referral practice from 1995 till 2006 were reviewed. Diagnosis was based on the presence of at least one segmentally sclerotic glomerulus, negative IF and extensive foot process effacement (>70%) without specific evidence of a secondary etiology. Biopsies were then classified by the Colombia Schema. Clinical history was reviewed and follow-up was classified as complete (CR) or partial remission (PR) of proteinuria, no remission (NR) or end stage renal disease (ESRD).
Results: 168 patients (92 male,74 female) met entry criteria. Average age was 42 ± 21 years (range 2 to 85) with 27 patients ≤ 18 year. 42 (25%) cases were African American and 86 (51%) were Caucasian, with ethnic origin other or not specified in the remaining patients. The frequency of FSGS variants was 13.7 % (N=23) COLL, 8.3% (N=14) CELL, 21.4% (N=36) TIP, 51.8 % (N=87) NOS, 4.8 % (N=8) PH. Black race showed more COLL and NOS compared to other variants and less in TIP. Edema and nephrotic proteinuria were present more in COLL and TIP. Hypertension and high serum creatinine at presentation were seen more in COLL and NOS. Outcome analysis of available data showed NR and ESRD more in COLL and CELL, compared to NOS and TIP. Conversely, NOS and TIP lesions had more PR or CR than other types. NOS was most common in children, and showed similar outcomes as in adults.
Conclusions: Our data support that different histopathologic variants have different clinical presentation and also different prognosis, regardless of age of patients.

1505 Prospective Assessment of C4d Deposits on Circulating Cells, Glomeruli, and Peritubular Capillaries in Lupus Nephritis (LN)

I Batal, S Bastacky, KV Liang, LP Kiss, T McHale, NL Wilson, B Paul, A Lertratanakul, JM Ahearn, SM Manzi, AH Kao. University of Pittsburgh, Pittsburgh, PA.
Background: Classical complement activation plays a key role in the pathogenesis of LN. Studies have suggested an association between C4d deposition in native renal tissue and LN severity. Cell-bound complement activation products have not been systematically studied in LN. We aimed to compare the C4d deposition on circulating cells and renal tissues between LN and non-systematic lupus erythematosus (SLE) renal disease controls and to determine the association of C4d deposition with LN class and disease activity.
Design: We prospectively evaluated 13 LN and 7 non-SLE renal control subjects who underwent renal biopsy. Concurrent C4d levels on circulating erythrocytes and platelets (EC4d, PC4d) were measured by flow cytometry. The distribution of immunoperoxidase C4d on formalin-fixed, paraffin-embedded renal biopsy tissues was semiquantitatively assessed (0-3; negative to diffuse) in peritubular capillaries (PTC) and glomeruli [GBM and/or mesangium]. LN histologic class, and activity (AI) and chronicity (CI) indices were assessed using the 2004 ISN/RPS classification and the NIH scoring systems, respectively.
Results: Six LN subjects (46%) had class IV [IV(S) (3) and IV(G) (3)]; the remainder had classes II (15%), III (23%) and/or V (38%). Median AI and CI were 6 and 2, respectively. Median EC4d levels of LN subjects were higher compared to controls (19.2 vs. 7.0, p=0.03). PC4d was detected in 6/13 (46%) LN subjects vs. 0/7 (0%) controls (p=0.05). EC4d level significantly correlated with LN AI (r=0.67, p=0.01). Furthermore, subjects with class IV LN had higher median EC4d levels compared to other classes (33.2 vs. 16.2, p=0.046). In renal tissues, mean glomerular C4d score was higher in LN (2.3+/-1.2) compared to controls (1.3+/-1.1, p=0.03), while PTC C4d score showed no significant difference. This C4d staining was associated with glomerular immune complex deposits. Neither glomerular nor PTC C4d score correlated with LN class or AI. Neither glomerular nor extraglomerular immune complex deposits correlated with EC4d levels.
Conclusions: This pilot study revealed that circulating cell and glomerular C4d levels were significantly higher in LN subjects compared to the non-SLE renal controls. In contrast to glomerular and PTC C4d, EC4d levels significantly correlated with LN disease activity. These findings suggest a potential role of C4d on circulating cells as a biomarker for LN.